Biotech Studies 34(SI), 9-17
http://doi.org/10.38042/biotechstudies.1677389

PROOF
RESEARCH PAPER

BIOTECH STUDIES

Green synthesis of silver nanoparticles using *Catalpa bignonioides* fruit

Emine Altınkaya[1]

[1]Manisa Celal Bayar University, Faculty of Engineering, Bioengineering Department, 45140 Muradiye, Yunusemre, Manisa, Türkiye

How to cite:
Altınkaya, E. (2025). Green synthesis of silver nanoparticles using Catalpa bignonioides fruit. *Biotech Studies*, *34*(SI), 9-17.
https://doi.org/10.38042/biotechstudies.1677389

Article History
Received 01 August 2024
Accepted 26 February 2025
First Online 15 April 2025

Corresponding Author
Tel.: +90 236 201 24 67
E-mail:
emine.altinkaya@cbu.edu.tr

Keywords
Medicinal plant extract
Metal nanoparticles
Antibacterial
Antioxidant
Ecofriendly approach

Abstract

For the first time, the aqueous extract of *Catalpa bignonioides* fruit was used as a reducing agent in the synthesis of silver nanoparticles with antibacterial and antioxidant properties by the green method. Physicochemical, antioxidant, and antibacterial properties of silver nanoparticles were investigated. The synthesized silver nanoparticles were characterized by UV–visible spectroscopy, Fourier transform infrared spectroscopy, X-ray diffraction, scanning electron microscope, and dynamic light scattering methods. The synthesis of silver nanoparticles was confirmed by red-brown color formation for visual observation. The surface plasmon resonance peak was observed at about 419 nm. The physicochemical test result shows that the average particle size of silver nanoparticles was between 22 and 31 nm. According to the antibacterial test results, silver nanoparticles exhibited good antibacterial properties by inhibiting the growth of gram-positive *Staphylococcus aureus* and gram-negative bacteria *Escherichia coli*. The 1,1-Diphenyl-2-picrylhydrazyl radical scavenging activity of the synthesized silver nanoparticles was investigated, and they exhibited antioxidant activity. Antibacterial and antioxidant silver nanoparticles have the potential to be used in textiles, cosmetics, food packaging, and biomedical applications.

Introduction

Noble metal nanoparticles, whose sizes generally vary between 1-100 nm, have become one of the most studied research topics recently due to their unique optical, electronic, mechanical, magnetic, and chemical properties (Forough & Farhadi, 2010; Horikoshi & Serpone, 2013). Silver nanoparticles are used in many areas such as photocatalytic organic dye degradation activity, chemical sensing, drug delivery, nanomedicine, antioxidants and antimicrobial agents, cell biology, agriculture, cosmetics, textiles, ointments, food industry, data storage (Ahmad et al., 2019). The emergence of multi-drug resistance to antibiotics used for microbial infections requires new antimicrobial compounds and modified treatment methods (Roy et al., 2019). In recent studies, nanomaterials have been developed to treat drug-resistant bacteria and cancer cells (Alavi et al., 2022; Khorsandi et al., 2021).

Although rapid production is achieved by using reducing chemical agents in synthesizing nanomaterials, the damage caused to the environment by toxic chemicals is quite high. To reduce the environmental damage caused by chemicals and to be economically affordable, the production of nanomaterials with green synthesis methods has been studied by many

researchers in recent years (Rafique et al., 2017). Green synthesis methods are important in nanoparticle synthesis due to the environmental problems caused by harmful chemical waste released into the environment (Roy et al., 2019). Many studies have been carried out on the use of plant extracts in obtaining nanoparticles using the green synthesis method (Ahmed et al., 2016; Shaik et al., 2018; Jalilian et al., 2020; Said et al., 2024; Ahmad et al., 2024).

Having high surface energy causes silver nanoparticles to agglomerate. Gums, polymers, cationic surfactants, and various plant extracts have been used to prevent agglomeration of nanoparticles. Capping agents surround the surface of nanoparticles and therefore play an important role in stabilization (Tanner et al., 2015; Restrepo & Villa, 2021). Plant metabolites are used as reducing and stabilizing agents for metal nanoparticle synthesis.

Catalpa bignonioides is frequently used in folk medicine and is known as the bean tree or cigarette tree (Munoz-Mingarro et al., 2003). *Catalpa bignonioides* is a folk remedy used in stomach diseases, bronchial diseases, and oncological diseases (Oh et al., 2021; Bozaci & Altinisik Tağaç, 2022). Researchers have used the valuable metabolites and different parts of catalpa for other purposes (Konyar, 2017; Oh et al., 2021; Bozaci & Altinisik Tağaç, 2022). *Catalpa bignonioides* extract contains metabolites such as flavonoids, oils, steroids, sugars, quinones, phenolic compounds, tannins, triterpenes, alkaloids, and iridoids (Oh et al., 2021). These metabolites are suitable candidates for nanoparticle synthesis.

This is the first time *Catalpa bignonioides* has been used as a reducing and capping agent in the green synthesis of silver nanoparticles. Non-toxic and economical silver nanoparticles were obtained by the green synthesis method. The physicochemical characterization of green synthesized silver nanoparticles was performed using X-ray diffraction analysis, Scanning Electron Microscopy, Attenuated Total Reflectance-Fourier Transform Infrared, Ultra-violet visible (UV-vis) spectroscopy, and Dynamic light scattering. Antibacterial properties were investigated against the Gram-positive bacteria *Staphylococcus aureus (S. aureus)* and Gram-negative bacteria *Escherichia coli* (*E. coli*); antioxidant activity was investigated using 1,1-Diphenyl-2-picrylhydrazyl (DPPH) free radical scavenging method.

Materials and Methods

Preparation of Chemicals

Silver nitrate (CAS No:7761-88-8) and NaOH (CAS No:1310-73-2) were purchased from Sigma Aldrich. 1 and 10 mM $AgNO_3$ solution was prepared for use in silver nanoparticle synthesis **(**AgNPs). $AgNO_3$ solutions were freshly prepared and used. 0.1 M NaOH solution was prepared for pH adjustment and stored at +4˚C. Ultrapure water was used for the preparation of the solutions.

Preparation of Plant Material

Fresh fruits of *Catalpa bignonioides* (FCB) were collected from *Catalpa bignonioides* trees in Manisa Celal Bayar University İlhan Varank Campus in September. The collected FCB had completed seed formation and their shells were closed. The FCB used in this study were cylindrical, 20-30 cm long, and 6-8 mm wide. FCB were washed with tap water then with ultrapure water and dried at room temperature. Fresh FCB, which was green in color, turned brown after drying. The dried FCB were stored under room conditions in a cool and dry environment.

AgNPs were synthesized by the green synthesis method using FCB extraction. FCB extraction was prepared using the following steps. Dried FCB were cut into small pieces using a grinder. The maceration method was used for extraction (Momchev et al., 2020). 10 g of ground FCB was added to 100 ml of ultrapure water and stirred overnight at room temperature. The mixture was first filtered roughly and then centrifuged at 4000 rpm to remove impurities. Finally, the obtained extract was filtered with Whatman filter paper (Whatman Grade 44- 1444) and stored at +4˚C.

Synthesis of Silver Nanoparticles

AgNPs synthesis was carried out by revising the method used by Salayová et al. to obtain AgNPs via the green synthesis method (Salayová et al., 2021). 1 and 10 mM $AgNO_3$ solutions were used for the preparation of AgNPs. The extract and $AgNO_3$ solution were mixed at 1(FCB extract): 9($AgNO_3$) and adjusted to pH: 9 using 0.1 M NaOH. The mixture was added to the conical flask, kept in an ultrasonic water bath for half an hour, and then stirred at room temperature for 24 hours. AgNPs formation was confirmed by observing the color change of the mixture and using a UV-Vis spectrophotometer. AgNPs formation steps are shown in Figure 1. The mixture was centrifuged at 14000 rpm for 45 minutes. The precipitated particles were washed using ultrapure water and centrifuged again, and the precipitated AgNPs were dried in an oven at 60 °C.

Characterization of Silver Nano Particles

The formation of AgNPs was confirmed using various characterization methods. Surface Plasmon Resonance (SPR) characterization was achieved using a UV-Vis spectrophotometer (Perkin Elmer Lambda 35). Dynamic light scattering (DLS) methods were performed to analyze the particle size of AgNPs. DLS analysis was performed at 25˚C for 60 s. AgNPs were analyzed using Attenuated Total Reflectance-Fourier Transform Infrared (ATR-FTIR) (Perkin Elmer, Spectrum 100), with spectra obtained in the wavenumber range of 4000–400 cm^{-1} with 25 scans at 4 cm^{-1} resolution.

X-ray diffraction (XRD) analysis was performed to evaluate the crystallinity of AgNPs. Percentage

Figure 1. AgNPs synthesis steps using FCB.

crystallinity was calculated using the below equation (Rotaru et al., 2018) with Origin software:

Crystallinity (%) = [Area of crystalline peaks/Area of all peaks (crystalline+amorphous)] x 100

The XRD and FTIR analysis was carried out at Manisa Celal Bayar University Experimental Science Application and Research Center (DEFAM). Scanning Electron Microscopy (SEM) (FEI QUANTA 250 FEG) analysis was used to examine the morphology of AgNPs and measure their size. SEM analysis was performed at İYTE-MAM.

Antibacterial Activity of AgNPs

Kirby-Bauer disk diffusion method (Singh et al., 2023) was used to determine the antibacterial activity of AgNPs in the determination of antibacterial activity, *S. aureus* was used as gram-positive bacteria, and *E. coli* was used as gram-negative bacteria. *S. aureus* and *E. coli* were incubated in a nutrient medium for 15 hours at 37°C. Inoculation was carried out by the spread plate method. 10 µl of AgNPs solution was absorbed on 0.5 cm*0.5 cm filter papers, placed on the agar, and incubated at 37°C for 24 hours. The sizes of the zones formed after incubation were measured.

Gentamicin antibiotic (10 mg/ml) was used as a positive control and water was used as a negative control. 3 repetitions were performed for each test.

Antioxidant Assay of AgNPs

1,1-Diphenyl-2-picrylhydrazyl (DPPH) method was used to determine the antioxidant activity of AgNPs. AgNPs were investigated for DPPH radical scavenging activity (RSA). 1mM Butylated hydroxyanisole (BHA) was used as a positive control. RSA was calculated using the equation given below (Azarbani & Shiravand, 2020):

$$RSA = \frac{A_C - A_S}{A_C} * 100$$

A_C refers to the absorbance of the DPPH solution A_S refers to the absorbance of the DPPH solution in the presence of AgNPs. AgNPs were used directly from synthesized mediums.

Statistical Analysis

Studies were performed with 3 repetitions. The results were compared with one-way analysis of variance (ANOVA) and Tukey Test. If $P<0.05$, it was considered statistically significant.

Results & Discussion

Synthesis of Silver Nano Particles

One of the verification methods to confirm the formation of AgNPs is the color change of the mixture of plant extract and silver nitrate solution (Mahiuddin, et al., 2020). While the silver nitrate solution was initially colorless, the mixture of silver nitrate solution and FCB extract became colored at the end of the 12-hour reaction period. With the formation of AgNPs, the color of the mixture turns deep brown. It is shown in Figure 2. Mahiuddin et al. (2020) also stated in their study that a similar color change occurred due to AgNPs formation. The color change after silver nanoparticle formation may be due to surface excitation of the plasmon resonance phenomenon of silver (Alsammarraie et al., 2018). Barabadi et al. (2021) stated that secondary metabolites such as vitamins, enzymes, proteins, tannins, phenolic compounds, and flavonoids act as capping and reducing agents in metal nanoparticle synthesis. Roy et al. (2019) reported that metabolites found in plant extracts can reduce Ag^+ to Ag^0 and facilitate AgNP synthesis, but the exact mechanism of reduction is not yet clear. They also stated that metabolites affect the morphology, size, and size distribution of silver nanoparticles. Panáček et al. (2006) synthesized AgNPs using glucose, galactose, maltose, and lactose and then compared the obtained AgNPs in

terms of size and antimicrobial activity. They concluded that AgNPs synthesized using maltose and lactose were smaller in size than those obtained using glucose and galactose. They also stated that smaller AgNPs exhibited higher antimicrobial activity.

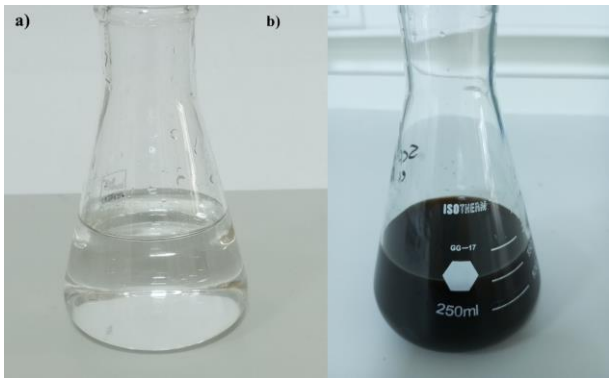

Figure 2. Image of a) Silver nitrate solution, b) mixture of silver nitrate and FCB extract after 12 h reaction time.

UV-Vis absorption spectra of silver nanoparticles synthesized with 1mM $AgNO_3$ (AgNP-1) and 10mM $AgNO_3$ (AgNP-10) were indicated in Figure 3. SPR distinct bands were observed at around 415 nm and 419 nm for AgNP-1 and AgNP-10, respectively. In the studies on silver nanoparticle synthesis via green synthesis, the surface plasmon resonances band of the synthesized nanoparticles was observed between 410-430 nm (Asif et al., 2022; Katta and Dubey, 2021; Widatalla et al., 2022; Panda et al., 2021). Accordingly, the surface plasmon resonance bands obtained for AgNP-1 and AgNP-10 are in the range of 410-430 nm, confirming the formation of AgNPs. The SPR band of AgNP-1 is smaller than the SPR band of AgNP-10 however, there is no significant difference between them. The absorbance value of the AgNP-10 is 1.2 while AgNP-1 is 0.85. Figure 3 shows that higher $AgNO_3$ concentration exhibited higher absorbance intensity.

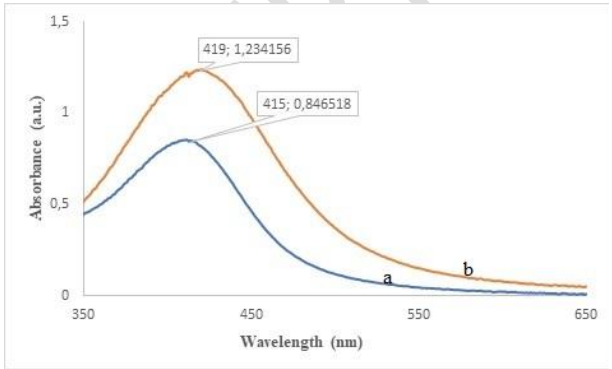

Figure 3. UV-Vis absorption spectra of biosynthesized silver nanoparticles with a) AgNP-1and b) AgNP-10.

Characterization of Silver Nano Particles

DLS Analysis

The green synthesized AgNPs were also confirmed by using the DLS method. The size and size distributions of AgNP-1 and AgNP-10 are indicated in Figure 4 and Figure 5, respectively. In Figure 4, there are 3 bands representing different-sized nanoparticle distributions for AgNP-1. According to the results shown by the DLS graph, the average size of AgNP-1 is 159.1 nm. The first band represents AgNP-1 which is 55 nm and has a ratio of 30%. In Figure 5, there are three bands for AgNP-10. Figure 5 indicates that the average size of AgNP-10 is 141.9 nm. The first band expresses AgNP-10 which is 41.91 nm and has a ratio of 13.1%.

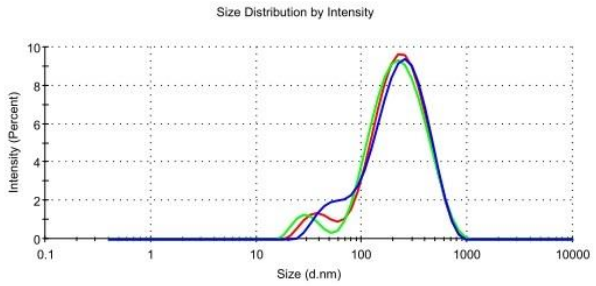

Figure 4. DLS graph of AgNP-1.

The larger particle size measured in the DLS method may be due to Brownian motion. DLS method measures the hydrodynamic size of metal nanoparticles. Hydrodynamic size measurement is calculated by measuring the electrostatic potential diameter around the metal nanoparticle in addition to the actual size. Therefore, the particle sizes obtained using the DLS method are larger than the particle sizes obtained as a result of other analysis methods such as SEM, XRD, and transmission electron microscopy (TEM) (Patil & Chougale, 2021). Although the DLS method shows larger nanoparticle sizes, thanks to its quick and accessible features, it provides a rapid prediction of particle sizes.

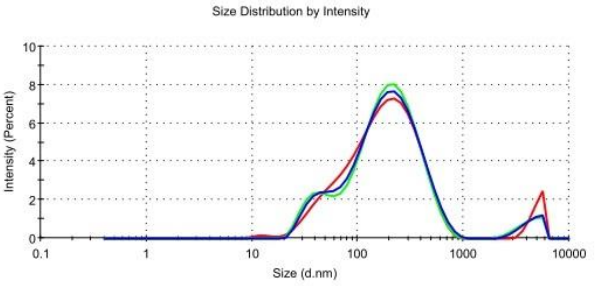

Figure 5. DLS graph of AgNP-10.

FTIR Analysis

FTIR method was used to identify the formation of silver nanoparticles by using an extract of *Catalpa bignonioides* fruit. FTIR spectra of *Catalpa bignonioides* fruit and AgNPs were compared, and differences were evaluated. FTIR spectrum of *Catalpa bignonioides* and green synthesized AgNPs are given in Figure 6. Significant differences in the FTIR spectra are noticeable at first glance.

Urnukhsaikhan et al. (2021) stated that the bands located between 3418 and 3429 cm^{-1} and around 1618 cm^{-1} indicate the presence of flavonoids and phenolic compounds, and the band formed around 1021 cm^{-1} indicates the ether, ester, and carboxylic acid groups of metabolites that are effective in nanoparticle formation.

Similar spectrum bands were obtained in the FTIR spectrum of *Catalpa bignonioides* fruit in Figure 6. The FTIR spectrum of *Catalpa bignonioides* exhibited a broad absorption band at about 3408 cm^{-1}, indicating the -OH group. A sharp peak belonging to the C-H vibrations of methylene and methyl groups is observed at 2914 cm^{-1}. The vibration band at around 1722 cm^{-1} represents the carbonyl group. The distinct vibration band at around 1604 cm-1 indicates the aromatic C=C ring stretching (Chen et al., 2012). The vibration bands at 1235 cm^{-1} and about 1014 cm^{-1} represent the C–O stretching vibrations in alcohols, phenols, and ether/ester groups (Hesas et al., 2013; Geçgel et al., 2015).

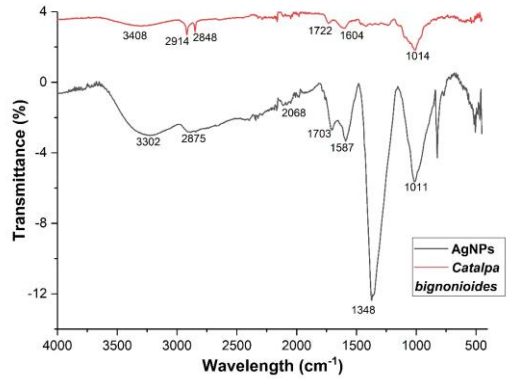

Figure 6. FTIR spectrum of AgNPs and *Catalpa bignonioides.*

When the FTIR spectrum of AgNPs is compared with the FTIR spectrum of *Catalpa bignonioides*, it is seen that some vibration bands are lost, and some are shifted. The vibration band at 3408 cm^{-1} shifted to 3302 cm^{-1} in the FTIR spectrum of AgNPs. The vibration band shifted from 2914 cm^{-1} to 2875 cm^{-1} and from 1014 cm^{-1} to 1011 cm^{-1} and the intensity of the band decreased. In addition, the vibration band at 1722 cm^{-1} shifted to 1703 cm^{-1}. The vibration bands at 2630, 2440, 2187, and 1235 cm^{-1} disappeared with the formation of AgNPs. Another piece of evidence supporting the formation of AgNPs may be the new peak appearing at 1348 cm^{-1}. Changes in FTIR spectra can be associated with AgNPs synthesis. Urnukhsaikhan et al. (2021) stated that changes in FTIR spectra confirm AgNPs synthesis.

XRD Analysis

XRD analysis was performed to investigate and confirm the crystalline structure of green synthesized silver nanoparticles. The XRD analysis is shown in Figure 7. Distinct peaks were observed at 29.27, 38.29, 44, 47.6, 64.7, and 77.6 2 theta (2θ) values. 38.29, 44, 64.7, and 77.6 2θ values correspond to diffraction planes (111), (200), (220), and (311), respectively. As stated in the studies of Asif et al. (2022); (111), (200), (220), and (311) diffraction planes show that the synthesized silver nanoparticles have a face-centered cubic (FCC) structure. The crystallinity index of AgNPs was calculated as 93.8%. The crystalline value of the synthesized AgNPs is quite high and the other impurity rate that may be present in the environment is low. Crystalline structures with diameters smaller than 100 nm form nanocrystalline structures (Hassanzadeh-Tabrizi, 2023). SEM analysis results show that AgNPs are smaller than 100 nm and therefore can be called nanocrystalline materials.

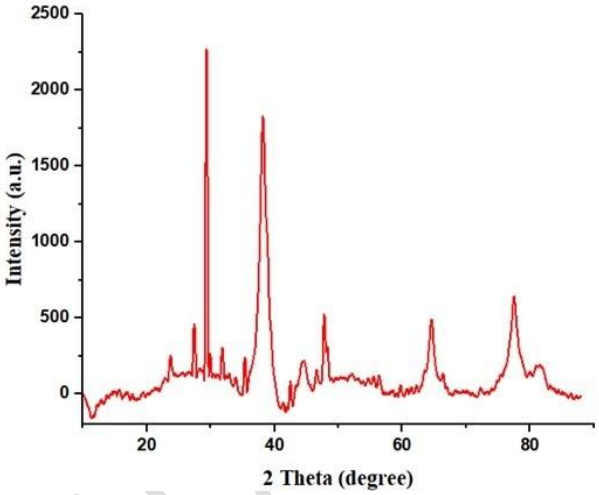

Figure 7. XRD graph of green synthesized AgNPs.

SEM Analysis

Histograms of AgNP-1 and AgNP-10 are indicated in Figure 8. Particle size and size distribution were calculated by ImageJ and Origin software. The 100.000-times magnified SEM image of AgNP-1 is given in Figure 8a. The 200.000-times magnified SEM image of AgNP-10 is given in Figure 8b. Histograms of AgNP-1 and AgNP-10 were indicated in Figure 8c and Figure 8d, respectively. The SEM images of both AgNP-1 and AgNP-10 include different particle sizes between 10-65 nm. The average particle size of AgNP-1 was calculated as 31.32±9 nm, and particle size distribution is shown in histogram Figure 8c. The average particle size of AgNP-10 was calculated as 22.3±5.6 nm and particle size distribution indicated in histogram Figure 8d. The average particle size of AgNP-10 is smaller than the average particle size of AgNP-1.

Particle size is important for nanoparticles. The size of inorganic nanoparticles affects their physical and chemical properties. Dolai et al. (2021) reported that when the particle size is larger than 100 nm, the probability of sedimentation will increase and as a result, the particle size will increase. They also stated that in biological studies, nanoparticles should be of appropriate particle size so that their interactions are not restricted. AgNP-1 and AgNP-10 have a particle size of approximately 20-30 nm. Since their particle size is <100 nm, they comply with the nanoparticle definition (Hassanzadeh-Tabrizi, 2023). The fact that their particle size is <100 nm largely eliminates the agglomeration problem and helps the nanoparticles to have a homogeneous size distribution. In Figures 8a and 8b, it is seen that the AgNPs distribution is homogeneous in most regions.

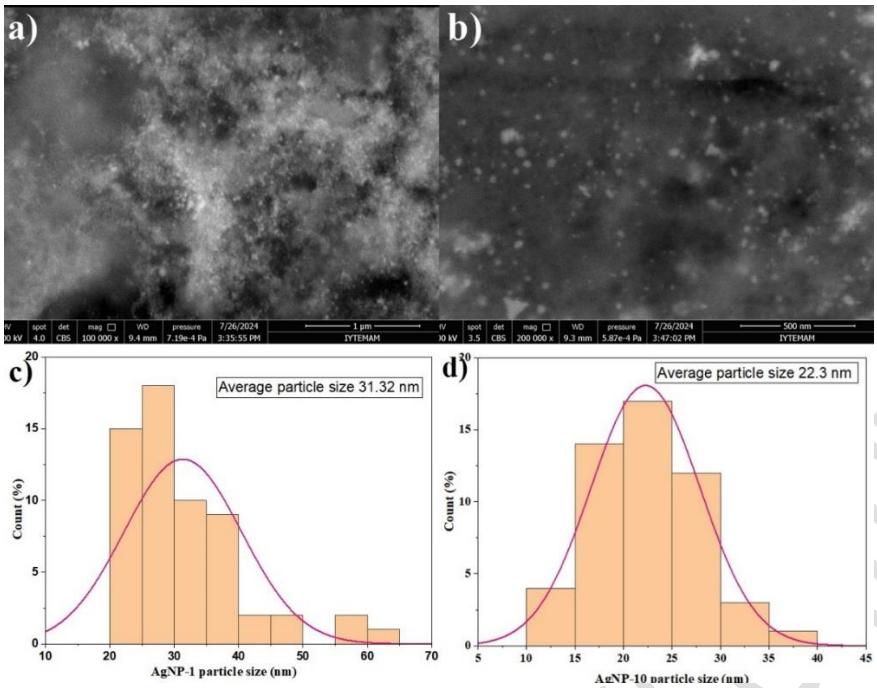

Figure 8. SEM images of AgNP-1 (a), AgNP-10 (b) and histogram of AgNP-1 (c) and AgNP-10 (d).

Antibacterial Activity

The inhibition capacity of AgNPs against *S. aureus and E. coli* bacteria was evaluated. The image of antibacterial activity is shown in Figure 9. Table 1 shows the zone diameters resulting from the inhibition of *S. aureus* and *E. coli* bacteria after 24 hours of incubation.

The AgNP-1 formed 8.7- and 8.7-mm zones for *E. coli* in both concentrations (4000 and 2000 µg/ml). The positive control created a zone diameter of 29 mm for *E. coli* bacteria. The AgNP-10 formed 10.7- and 9.7-mm zones for *E. coli* in both concentrations (4000 and 2000 µg/ml). Positive control created a zone diameter of 24 mm for *E. coli* bacteria.

The AgNP-1 formed 9.3- and 8-mm zones for *S. aureus in* both concentrations (4000 and 2000 µg/ml). The positive control created a zone diameter of 16 mm for *S. aureus* bacteria. The AgNP-10 formed 9.3- and 10-mm zones for *S. aureus* in both concentrations (4000 and 2000 µg/ml). The positive control created a zone diameter of 19 mm for *S. aureus* bacteria. Negative control bacteria inhibition zones are 0-mm for all results.

According to the results AgNP-1 and AgNP-10 exhibited antibacterial activity in both *S. aureus* and *E. coli* bacteria. The most effective antibacterial activity against *E. coli* was exhibited by 4000 µg/ml AgNP-10. The most effective antibacterial activity against *S. aureus* was exhibited by 2000 µg/ml AgNP-10. Considering the zone diameters, AgNP-10 exhibited more effective antibacterial activity than AgNP-1 for both *S. aureus* and *E. coli.* The smaller average particle diameter of AgNP-10 may have contributed to its greater antibacterial activity. Scientific research has shown that silver nanoparticles with smaller particle diameters have greater antibacterial activity because of having a larger surface area (Rajkumar et al., 2020; Menichetti et al., 2023). Martínez-Castañon et al. (2008) also reported that silver nanoparticles with smaller particle sizes exhibit better antibacterial activity. They stated that the small particle size allows silver nanoparticles to reach the nuclear content of bacteria more easily and that they can have more contact with bacteria due to their large surface area.

According to Table 1, no linear or inverse relationship was observed between AgNPs concentration and antibacterial activity. For *E. coli and S. aureus*, there is a significant difference among the zones formed by the samples and the positive control at 4000 and 2000 (µg/ml) AgNPs concentration (P<0.05).

Table 1. Antibacterial activity results of AgNP-1 and AgNP-10

Concentration of AgNPs (µg/ml)	*Escherichia coli*		*Staphylococcus aureus*	
	AgNP-1 Zone diameter (mm)	AgNP-10 Zone diameter (mm)	AgNP-1 Zone diameter (mm)	AgNP-10 Zone diameter (mm)
4000	8.7	10.7	9.3	9.3
2000	8.7	9.7	8	10
Negative control	0	0	0	0
Positive control	29	24	16	19

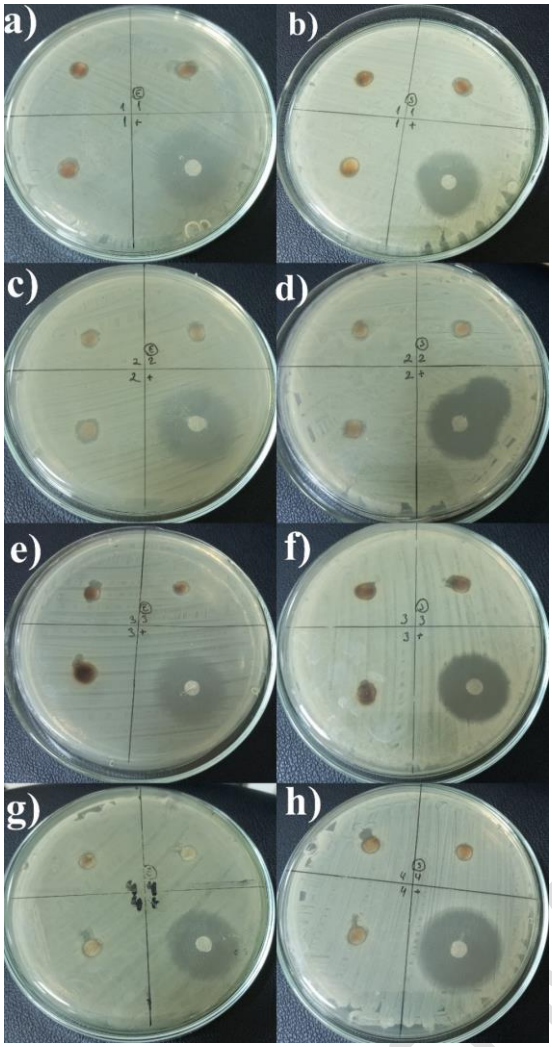

Figure 9. Antibacterial test results of AgNP-1 4000µg/ml [a) *E.coli*, b) *S. aureus*] and 2000 µg/ml [c) *E.coli*, d) *S. aureus*]; AgNP-10 4000µg/ml [e) *E.coli*, f) *S. aureus*] and 2000 µg/ml [g) *E.coli*, h) *S. aureus*].

Antioxidant Activity

The concentration-dependent antioxidant effects of the samples are shown in Figure 10. The results indicated that AgNPs have antioxidant activity. There is a linear proportion between the concentration ratio of the samples and the % antioxidant effect. For 1000 µl/ml concentration, AgNP-1 and AgNP-10 showed 46.29% and 50.7% maximum antioxidant activity, respectively. The maximum antioxidant activity of AgNP-10 is higher than the maximum antioxidant activity of AgNP-1. No significant difference was observed between AgNP-1 and AgNP-10 (P>0.05). Positive control exhibited 96.06% antioxidant activity while negative control didn't. There is a significant difference between AgNP-1 and concentration; AgNP-10 and concentration; positive control and concentration; positive control and AgNP-1; positive control and AgNP-10 (P<0.05).

Dilshad et al. (2020) stated in their study that the antioxidant activity of AgNPs may be due to the coating agents surrounding the silver ions. In the formation of AgNPs with green synthesis, the coating agents surrounding the silver ions may exhibit antioxidant activity due to their metal-chelating properties. AgNP-1 and AgNP-10 exhibited 46% and 50% antioxidant activity, respectively, according to the DPPH method. AgNP-1 and AgNP-10 have an average particle size of 31.32 nm and 22.3 nm, respectively. The fact that the antioxidant activity of AgNP-10 is slightly higher than AgNP-1 may be due to its smaller particle size. Since AgNP-10 has a larger surface area, more coating agents can be adsorbed around the silver ions. Thus, the nanoparticle with more coating agents on its surface may have exhibited more antioxidant effects. Although there is a small difference of 9 nm between the average particle sizes of AgNP-1 and AgNP-10, the difference in their antioxidant activities is approximately 4%.

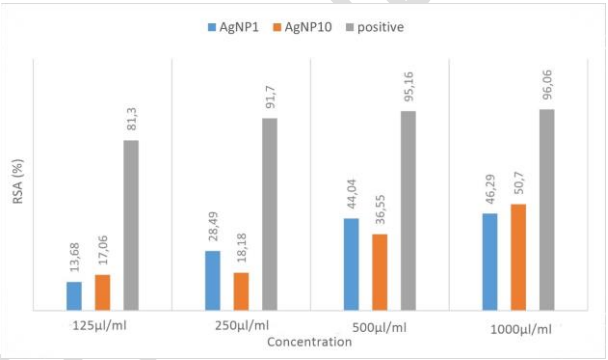

Figure 10. Antioxidant activity of AgNP-1, AgNP-10, and positive control.

Conclusion

Silver nanoparticles were synthesized by the green synthesis method using an aqueous extract of *Catalpa bignonioides* fruit. Characterization methods have revealed results confirming the synthesis of AgNPs. According to the results, using *Catalpa bignonioides* fruit aqueous extract as a reducing and capping agent in the synthesis of AgNPs is a very effective method. The average size of the synthesized AgNPs is 31.32 nm for AgNP-1 and 22.3 nm for AgNP-10 according to the result of SEM analysis. Significant changes in the FTIR spectrum also confirm the formation of AgNPs. XRD results indicated that synthesized AgNPs have a face-centered cubic (FCC) structure. The crystalline index of AgNPs was obtained as 93.8%. AgNPs showed antibacterial activity, with AgNP-10 having greater antibacterial activity than AgNP-1. AgNPs showed antioxidant activity, the activity is obtained with AgNP-10. AgNPs produced from *Catalpa bignonioides* fruit have the potential to be used in textile, cosmetics, food packaging, and biomedical applications.

Funding Information

This research received no specific grant from any funding agency in the public, commercial, or not-for-profit sectors.

Author Contributions

The author confirms sole responsibility for the following: study conception and design, data collection, analysis and interpretation of results, and manuscript preparation.

Acknowledgements

The author thanks to Ayşegül İnam (MSc, Manisa Celal Bayar University) and Tuğçe Mutaf Kılıç (MSc, Manisa Celal Bayar University) for their support.

References

Ahmad, M. Z., Saeed, A. M., Elnoubi, O. A., Alasiri, A. S., Abdel-Wahab, B. A., Alqahtani, A. A., Pathak, K., Saikia, R., Kakoti, B. B., & Das, A. (2024). Chitosan-based topical formulation integrated with green-synthesized silver nanoparticles utilizing Camellia sinensis leaf extracts: A promising approach for managing infected wounds. *International Journal of Biological Macromolecules*, *257*, 128573. https://doi.org/10.1016/j.ijbiomac.2023.128573

Ahmad, S., Munir, S., Zeb, N., Ullah, A., Khan, B., Ali, J., Bilal, M., Omer, M., Alamzeb, M., Salman, S M., & Ali, S. (2019). Green nanotechnology: A review on green synthesis of silver nanoparticles—An ecofriendly approach. *International journal of nanomedicine*, 5087-5107. https://doi.org/10.2147/IJN.S200254

Ahmed, S., Ahmad, M., Swami, B. L., & Ikram, S. (2016). Green synthesis of silver nanoparticles using Azadirachta indica aqueous leaf extract. *Journal of radiation research and applied sciences*, *9*(1), 1-7. https://doi.org/10.1016/j.jrras.2015.06.006

Alavi, M., Rai, M., Martinez, F., Kahrizi, D., Khan, H., Rose Alencar De Menezes, I., Coutinho, H. D., & Costa, J. G. M. (2022). The efficiency of metal, metal oxide, and metalloid nanoparticles against cancer cells and bacterial pathogens: different mechanisms of action. *Cellular, Molecular and Biomedical Reports*, *2*(1), 10-21. https://doi.org/10.55705/cmbr.2022.147090.1023

Alsammarraie, F. K., Wang, W., Zhou, P., Mustapha, A., & Lin, M. (2018). Green synthesis of silver nanoparticles using turmeric extracts and investigation of their antibacterial activities. *Colloids and Surfaces B: Biointerfaces*, *171*, 398-405. https://doi.org/10.1016/j.colsurfb.2018.07.059

Asif, M., Yasmin, R., Asif, R., Ambreen, A., Mustafa, M., & Umbreen, S. (2022). Green synthesis of silver nanoparticles (AgNPs), structural characterization, and their antibacterial potential. *Dose-Response*, *20*(2), 15593258221088709. https://doi.org/10.1177/15593258221088709

Azarbani, F., & Shiravand, S. (2020). Green synthesis of silver nanoparticles by Ferulago macrocarpa flowers extract and their antibacterial, antifungal and toxic effects. *Green Chemistry Letters and Reviews*, *13*(1), 41-49. https://doi.org/10.1080/17518253.2020.1726504

Barabadi, H., Mojab, F., Vahidi, H., Marashi, B., Talank, N., Hosseini, O., & Saravanan, M. (2021). Green synthesis, characterization, antibacterial and biofilm inhibitory activity of silver nanoparticles compared to commercial silver nanoparticles. *Inorganic Chemistry Communications*, *129*, 108647. https://doi.org/10.1016/j.inoche.2021.108647

Bozaci, E., & Altınışık Tağaç, A. (2022). Extraction and characterization of new cellulosic fiber from Catalpa bignonioides fruits for potential use in sustainable products. *Polymers*, *15*(1), 201. https://doi.org/10.3390/polym15010201

Chen, Y., Mastalerz, M., & Schimmelmann, A. (2012). Characterization of chemical functional groups in macerals across different coal ranks via micro-FTIR spectroscopy. *International Journal of Coal Geology, 104*, 22-33. https://doi.org/10.1016/j.coal.2012.09.001

Dilshad, E., Bibi, M., Sheikh, N. A., Tamrin, K. F., Mansoor, Q., Maqbool, Q., & Nawaz, M. (2020). Synthesis of functional silver nanoparticles and microparticles with modifiers and evaluation of their antimicrobial, anticancer, and antioxidant activity. *Journal of functional biomaterials, 11*(4), 76. https://doi.org/10.3390/jfb11040076

Dolai, J., Mandal, K., & Jana, N. R. (2021). Nanoparticle size effects in biomedical applications. *ACS Applied Nano Materials*, *4*(7), 6471-6496. https://doi.org/10.1021/acsanm.1c00987

Forough, M., & Farhadi, K. (2010). Biological and green synthesis of silver nanoparticles. *Turkish Journal of Engineering and Environmental Sciences*, *34*(4), 281-287. https://doi.org/10.3906/muh-1005-30

Geçgel, Ü., Kocabıyık, B., & Üner, O. (2015). Adsorptive removal of methylene blue from aqueous solution by the activated carbon obtained from the fruit of catalpa bignonioides. *Water, Air, & Soil Pollution*, *226*, 1-14. https://doi.org/10.1007/s11270-015-2513-4

Hassanzadeh-Tabrizi, S. A. (2023). Precise calculation of crystallite size of nanomaterials: A review. *Journal of Alloys and Compounds*, 171914. https://doi.org/10.1016/j.jallcom.2023.171914

Hesas, R. H., Niya, A. A., Daud, W. M. A. W., & Sahu, J. N. (2013). Preparation of granular activated carbon from oil palm shell by microwave-induced chemical activation: optimization using surface response methodology. *Chemical Engineering Research and Design, 91*, 2447–2456. https://doi.org/10.1016/j.cherd.2013.06.004

Horikoshi, S., & Serpone, N. (Eds.). (2013). *Microwaves in nanoparticle synthesis: fundamentals and applications* (pp. 1-24). John Wiley & Sons. https://doi.org/10.1002/9783527648122.ch1

Jalilian, F., Chahardoli, A., Sadrjavadi, K., Fattahi, A., & Shokoohinia, Y. (2020). Green synthesized silver nanoparticle from Allium ampeloprasum aqueous extract: Characterization, antioxidant activities, antibacterial and cytotoxicity effects. *Advanced Powder Technology*, *31*(3), 1323-1332. https://doi.org/10.1016/j.apt.2020.01.011

Katta, V. K. M., & Dubey, R. S. (2021). Green synthesis of silver nanoparticles using Tagetes erecta plant and investigation of their structural, optical, chemical and morphological properties. *Materials Today: Proceedings*, *45*, 794-798. https://doi.org/10.1016/j.matpr.2020.02.809

Khorsandi, K., Hosseinzadeh, R., Sadat Esfahani, H., Keyvani-Ghamsari, S., & Ur Rahman, S. (2021). Nanomaterials as drug delivery systems with antibacterial properties:

current trends and future priorities. *Expert Review of Anti-infective Therapy*, *19*(10), 1299-1323. https://doi.org/10.1080/14787210.2021.1908125

Konyar, S. T. (2017). An Overview of Pollen and Anther Wall Development in Catalpa bignonioides Walter (BIGNONIACEAE). *Trakya University Journal of Natural Sciences*, *18*(2), 123-132. https://doi.org/10.23902/trkjnat.309718

Mahiuddin, M., Saha, P., & Ochiai, B. (2020). Green synthesis and catalytic activity of silver nanoparticles based on Piper chaba stem extracts. *Nanomaterials*, *10*(9), 1777. https://doi.org/10.3390/nano10091777

Martínez-Castañon, G. A., Nino-Martinez, N., Martinez-Gutierrez, F., Martínez-Mendoza, J. R., & Ruiz, F. (2008). Synthesis and antibacterial activity of silver nanoparticles with different sizes. *Journal of nanoparticle research*, *10*, 1343-1348. https://doi.org/10.1007/s11051-008-9428-6

Menichetti, A., Mavridi-Printezi, A., Mordini, D., & Montalti, M. (2023). Effect of size, shape and surface functionalization on the antibacterial activity of silver nanoparticles. *Journal of Functional Biomaterials*, *14*(5), 244. https://doi.org/10.3390/jfb14050244

Momchev, P., Ciganović, P., Jug, M., Marguí, E., Jablan, J., & Zovko Končić, M. (2020). Comparison of maceration and ultrasonication for green extraction of phenolic acids from Echinacea purpurea aerial parts. *Molecules*, *25*(21), 5142. https://doi.org/10.3390/molecules25215142

Munoz-Mingarro, D., Acero, N., Llinares, F., Pozuelo, J. M., de Mera, A. G., Vicenten, J. A., Morales, L., Alguacil, L. F., & Pérez, C. (2003). Biological activity of extracts from Catalpa bignonioides Walt. (Bignoniaceae). *Journal of Ethnopharmacology*, *87*(2-3), 163-167. https://doi.org/10.1016/S0378-8741(03)00111-9

Oh, Y., Lee, D., Park, S., Kim, S. H., & Kang, K. S. (2021). The chemical constituents from fruits of *Catalpa bignonioides* Walt. and their α-glucosidase inhibitory activity and insulin secretion effect. *Molecules*, *26*(2), 362. https://doi.org/10.3390/molecules26020362

Panáček, A., Kvítek, L., Prucek, R., Kolář, M., Večeřová, R., Pizúrová, N., Sharma, V. K., Nevěčná, T., & Zbořil, R. (2006). Silver colloid nanoparticles: synthesis, characterization, and their antibacterial activity. *The Journal of Physical Chemistry B*, *110*(33), 16248-16253. https://doi.org/10.1021/jp063826h

Panda, M. K., Dhal, N. K., Kumar, M., Mishra, P. M., & Behera, R. K. (2021). Green synthesis of silver nanoparticles and its potential effect on phytopathogens. *Materials Today: Proceedings*, *35*, 233-238. https://doi.org/10.1016/j.matpr.2020.05.188

Patil, R. B., & Chougale, A. D. (2021). Analytical methods for the identification and characterization of silver nanoparticles: A brief review. *Materials Today: Proceedings*, *47*, 5520-5532. https://doi.org/10.1016/j.matpr.2021.03.384

Rafique, M., Sadaf, I., Rafique, M. S., & Tahir, M. B. (2017). A review on green synthesis of silver nanoparticles and their applications. *Artificial cells, nanomedicine, and biotechnology*, *45*(7), 1272-1291. https://doi.org/10.1080/21691401.2016.1241792

Rajkumar, P. V., Prakasam, A., Rajeshkumar, S., Gomathi, M., Anbarasan, P. M., & Chandrasekaran, R. (2020). Green synthesis of silver nanoparticles using Gymnema sylvestre leaf extract and evaluation of its antibacterial activity. *South African Journal of Chemical Engineering*, *32*(1), 1-4. https://hdl.handle.net/10520/EJC-1d7a3051f1

Restrepo, C. V., & Villa, C. C. (2021). Synthesis of silver nanoparticles, influence of capping agents, and dependence on size and shape: A review. *Environmental Nanotechnology, Monitoring & Management*, *15*, 100428. https://doi.org/10.1016/j.enmm.2021.100428

Rotaru, R., Savin, M., Tudorachi, N., Peptu, C., Samoila, P., Sacarescu, L., & Harabagiu, V. (2018). Ferromagnetic iron oxide–cellulose nanocomposites prepared by ultrasonication. *Polymer chemistry*, *9*(7), 860-868. https://doi.org/10.1039/C7PY01587A

Roy, A., Bulut, O., Some, S., Mandal, A. K., & Yilmaz, M. D. (2019). Green synthesis of silver nanoparticles: biomolecule-nanoparticle organizations targeting antimicrobial activity. *RSC advances*, *9*(5), 2673-2702. https://doi.org/10.1039/C8RA08982E

Said, A., Abu-Elghait, M., Atta, H. M., & Salem, S. S. (2024). Antibacterial activity of green synthesized silver nanoparticles using Lawsonia inermis against common pathogens from urinary tract infection. *Applied Biochemistry and Biotechnology*, *196*(1), 85-98. https://doi.org/10.1007/s12010-023-04482-1

Salayová, A., Bedlovičová, Z., Daneu, N., Baláž, M., Lukáčová Bujňáková, Z., Balážová, Ľ., & Tkáčiková, Ľ. (2021). Green synthesis of silver nanoparticles with antibacterial activity using various medicinal plant extracts: Morphology and antibacterial efficacy. *Nanomaterials*, *11*(4), 1005. https://doi.org/10.3390/nano11041005

Shaik, M. R., Khan, M., Kuniyil, M., Al-Warthan, A., Alkhathlan, H. Z., Siddiqui, M. R. H., Shaik, J. P., Ahamed, A., Mahmood, A., Khan, M., & Adil, S. F. (2018). Plant-extract-assisted green synthesis of silver nanoparticles using Origanum vulgare L. extract and their microbicidal activities. *Sustainability, 10*(4), 913. https://doi.org/10.3390/su10040913

Singh, C., Anand, S. K., Upadhyay, R., Pandey, N., Kumar, P., Singh, D., Tiwari, P., Saini, R., Tiwari, K. N., Mishra, S. K., & Tilak, R. (2023). Green synthesis of silver nanoparticles by root extract of Premna integrifolia L. and evaluation of its cytotoxic and antibacterial activity. *Materials Chemistry and Physics, 297*, 127413. https://doi.org/10.1016/j.matchemphys.2023.127413

Tanner, E. E., Tschulik, K., Tahany, R., Jurkschat, K., Batchelor-McAuley, C., & Compton, R. G. (2015). Nanoparticle capping agent dynamics and electron transfer: polymer-gated oxidation of silver nanoparticles. *The Journal of Physical Chemistry C*, *119*(32), 18808-18815. https://doi.org/10.1021/acs.jpcc.5b05789

Urnukhsaikhan, E., Bold, B. E., Gunbileg, A., Sukhbaatar, N., & Mishig-Ochir, T. (2021). Antibacterial activity and characteristics of silver nanoparticles biosynthesized from Carduus crispus. *Scientific Reports*, *11*(1), 21047. https://doi.org/10.1038/s41598-021-00520-2

Widatalla, H. A., Yassin, L. F., Alrasheid, A. A., Ahmed, S. A. R., Widdatallah, M. O., Eltilib, S. H., & Mohamed, A. A. (2022). Green synthesis of silver nanoparticles using green tea leaf extract, characterization and evaluation of antimicrobial activity. *Nanoscale Advances*, *4*(3), 911-915. https://doi.org/10.1039/D1NA00509J